

## Chapter 4

---

### DIODES AND ELECTRON GUNS

---

---

The simplest vacuum tube is the two-electrode tube, or diode. In its usual form, this tube consists of a thermionic cathode and an anode. When the anode is at a positive potential with respect to the cathode, electrons emitted from the cathode are drawn to the anode, and when the anode is negative with respect to the cathode, virtually no electrons reach it. The diode therefore serves as a one-way current device, and as such it finds its chief application.

The diode geometry that lends itself most readily to analysis of the electron behavior is that in which the cathode and anode are planar, parallel, and of linear dimensions large compared with the spacing between them. We shall find that the significant laws that describe the operation of diodes with this type of geometry apply also to diodes with more complicated geometries.

If a small aperture is made in the anode of a planar diode, some of the electrons emitted from the cathode pass through the aperture into the space beyond. The device therefore acts as a crude sort of electron gun. Most electron guns use at least one additional electrode which helps to shape the field between the cathode and anode. With a suitable choice of geometry for this electrode, and with a suitable shape of cathode and anode, it is possible to cause essentially all the current drawn from the cathode to pass through the anode aperture.

Electron guns are a basic element in many types of electron tubes. Many microwave tubes make use of high-current-density, cylindrical beams of electrons. To obtain these beams, electrode geometries must be devised that accelerate the electrons to the required velocity and focus them to the required beam diameter. The electron guns used in cathode-ray tubes and storage tubes focus the beam to a "crossover," and an electron lens beyond the crossover forms an image of the crossover on the screen or storage

surface of the tube. Several designs of electron guns for microwave tubes, cathode-ray tubes, and storage tubes are described in Section 4.5.

Because the electrons emitted from the cathode of an electron gun have a finite component of velocity parallel to the cathode at the time of emission, the electrons tend to drift across the beam while being accelerated away from the cathode. If the electron beam is focused to a smaller diameter than that of the cathode, the transverse velocities of the electrons in the beam increase as the beam diameter is decreased. Ultimately, if the beam is focused to a crossover, the maximum current density that can be obtained at the crossover for a given cathode current density and beam voltage is limited by the emission velocities at the cathode. These effects are discussed in Section 4.4.

In this chapter and in subsequent chapters we shall use the subscript  $o$  to designate dc electrode voltages and currents. Thus  $V_{ao}$  and  $I_{ao}$  are the dc anode voltage and current.

## 4.1 The Planar Diode

Here we consider a diode consisting of two planar, parallel electrodes of linear dimensions large compared with the spacing between them. We assume that the effects of fringing fields at the edges of the electrodes can be neglected, and that the fields between the electrodes are everywhere normal to the electrodes.

Figure 4.1-1 shows qualitatively the fields and potential distribution<sup>1</sup> in the interelectrode space of such a tube for several conditions of applied anode voltage and cathode emission current. When electrons are present in the interelectrode space, electric field lines extend from induced positive charges on the electrodes to the electrons, and *the net positive charge on the electrodes is equal to the total negative charge in the interelectrode space*. In Figure 4.1-1(a), the anode is held at cathode or ground potential while appreciable electron emission from the cathode takes place. (We assume that both electrodes have the same work function, so that the effects of contact potential difference can be neglected.) In this case, electric field lines extend from induced positive charges on both electrodes to the electrons in the interelectrode space, with the result that the potential in the space between the electrodes is less than ground potential and reaches a minimum at some

---

<sup>1</sup>Notice that in Figures 2.1-2 and 2.1-3 of Chapter 2 we have plotted the potential that applies to a negative unit charge, whereas in Figure 4.1-1 we plot the potential of a positive unit charge. In the field of atomic physics, convention calls for using the potentials that apply to negative charges, whereas in electron-tube work the potentials that apply to positive charges are more frequently used.

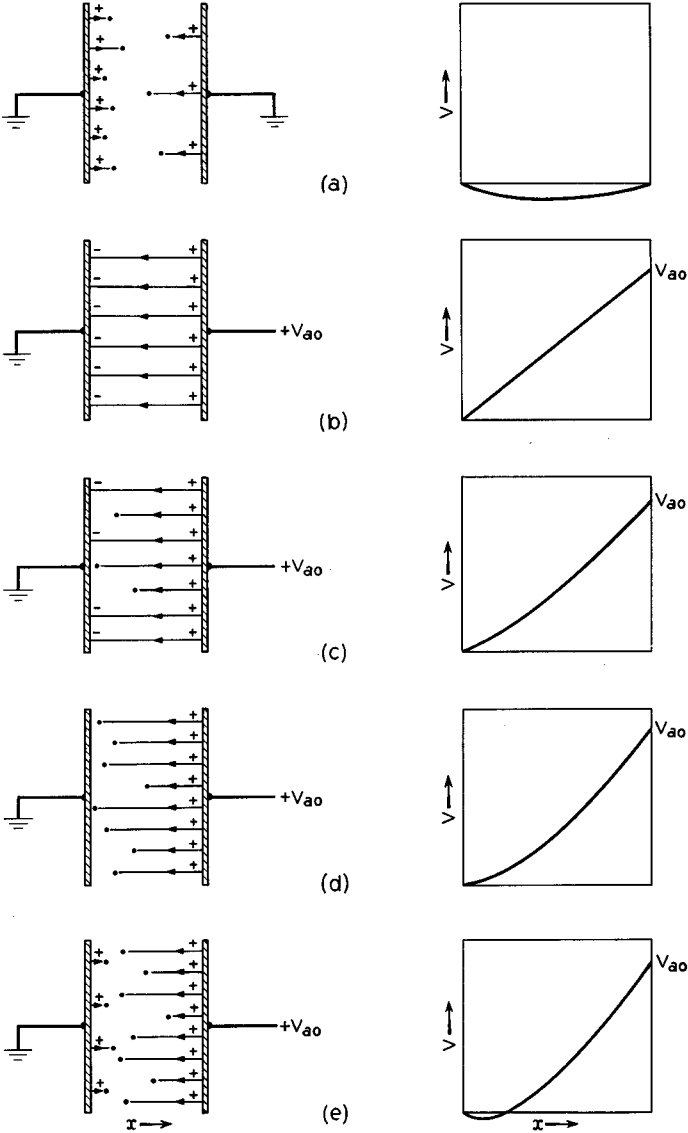


FIG. 4.1-1 The field lines and potential distribution in the interelectrode space of a planar diode for several conditions of applied anode voltage and cathode emission current.

point between the electrodes. Since the electrons emitted from the cathode have a range of velocities, the faster electrons are able to overcome the potential minimum and pass on to the anode, whereas those emitted with relatively small velocity travel only part way out to the potential minimum before being returned to the cathode.

To the right of the potential minimum, all the electrons move from left to right, whereas to the left of the potential minimum there are additional electrons that travel part way out to the potential minimum and return to the cathode. This means that the electron density to the left of the potential minimum is greater than the electron density at points of equal potential to the right of the potential minimum. Consequently, the potential gradient is greater to the left of the potential minimum, and the position of the potential minimum is displaced to the left of the mid-point between the electrodes. Later we shall find that the potential difference between the cathode and the potential minimum is directly proportional to the average electron emission energy in the direction normal to the cathode. (See Equation (4.1-1).)

In Figure 4.1-1(b), a voltage  $V_{ao}$  is assumed to be applied to the anode, but no cathode emission takes place. In this case, field lines extend from positive charges on the anode to negative charges on the cathode, and the potential varies linearly from the cathode to the anode. In Figure 4.1-1(c), a small cathode emission is also assumed to take place. In this case, the emitted electrons experience a field which draws them toward the anode, so that the entire cathode emission current reaches the anode. The current drawn from the cathode is then said to be temperature-limited, since its magnitude is determined by the cathode temperature and shows little variation with changes in positive anode potential. The density of field lines leaving the anode in this case is greater than in Figure 4.1-1(b), whereas the density of field lines arriving at the cathode is less than in Figure 4.1-1(b), the same anode voltage being applied in each case. (The density of field lines at a given point is, of course, proportional to the potential gradient at that point.)

As the cathode temperature is raised so that more electrons are emitted, more field lines originating on the anode terminate on electrons in the inter-electrode space, and the electric field intensity at the cathode surface decreases correspondingly. At a sufficiently high cathode temperature, the field lines extending from the anode to electrons in the interelectrode space have sufficient density to account for the potential drop  $V_{ao}$ , and the electric field intensity at the cathode is zero. This condition is illustrated in Figure 4.1-1(d). With still greater cathode emission (Figure 4.1-1(e)), a potential minimum forms in front of the cathode, and some of the emitted electrons are returned to the cathode.

When a potential minimum is present in front of the cathode, changes in cathode temperature serve only to raise or lower the potential at the minimum and have very little effect on the net current drawn from the cathode. The current drawn from the cathode in this case is said to be space-charge-limited and is determined largely by the voltage applied to the anode. Increasing the anode voltage requires a greater density of field lines at the anode to account for the potential difference between the anode and the potential minimum. This means that more field lines extend from the anode to the electrons in the interelectrode space, and more of the emitted electrons are drawn to the anode. Thus with increasing anode voltage, the current drawn from the cathode increases, and the potential at the minimum rises closer to cathode potential. At a sufficiently high anode potential, the potential minimum disappears, and the current drawn from the cathode becomes temperature-limited.

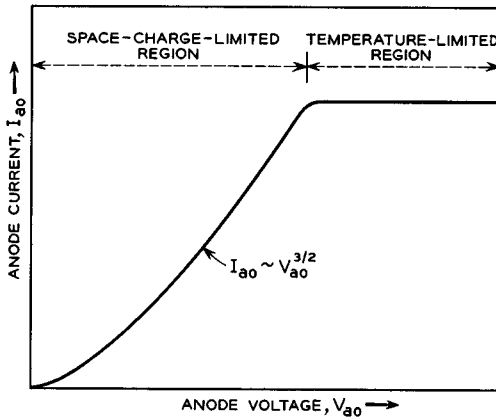


FIG. 4.1-2 An idealized plot of anode current vs. anode voltage for a planar diode. The cathode temperature is assumed to be fixed.

Figure 4.1-2 shows an idealized plot of anode current vs. anode voltage for a planar diode. The regions in which the current drawn to the anode is space-charge-limited and temperature-limited are shown in the figure. A planar diode with a tungsten cathode would exhibit a current-voltage relationship that would closely approximate this curve.

From the discussion of emission energies given in Section 2.4, it will be recalled that the fraction  $F$  of the emitted electrons that can overcome a retarding voltage of  $V$  volts is given by  $F = e^{-eV/kT}$ . Thus, when the current drawn from the cathode of a diode is space-charge-limited, the fraction  $F$  of the total emission current that is drawn to the anode is given by  $F =$

$\epsilon^{-eV_m/kT}$ , where  $-V_m$  is the potential at the potential minimum measured relative to cathode potential. Hence

$$V_m = -\frac{kT}{e} \ln F = -\frac{T}{11,600} \ln F \text{ volts} \quad (4.1-1)$$

For  $F = 1/\epsilon$  and  $T = 1160^\circ\text{K}$ ,  $V_m = 0.1$  volt. Under most operating conditions,  $V_m$  is of the order of a few tenths of a volt or less. It is noteworthy that  $V_m$  is directly proportional to  $kT$ , the average emission energy in the direction normal to the cathode. If the emission energy were zero, the potential minimum would vanish.

The plane of the potential minimum is often called the virtual cathode, since all the electrons that pass this plane ultimately reach the anode. Let us now proceed to determine the current-voltage relationship for a space-charge-limited planar diode. We shall assume that the electrons pass the virtual cathode with zero velocity. The potential at the virtual cathode is taken to be zero, and distance  $x$  is measured from the virtual cathode toward the anode. If  $V(x)$  is the potential at a point  $x$  meters from the virtual cathode, and  $u(x)$  is the electron velocity at that point, the boundary conditions at  $x = 0$  are  $V = 0$ ,  $u = 0$ , and  $dV/dx = 0$ . The equations relating the parameters of interest are:

Poisson's Equation

$$\frac{d^2V}{dx^2} = -\frac{\rho}{\epsilon_0} \quad (4.1-2)$$

the energy equation

$$\frac{1}{2}mu^2 = eV \quad (4.1-3)$$

and the current density relation

$$J = -\rho u \quad (4.1-4)$$

where  $\rho$  is the volume charge density.

In these equations,  $\rho$ ,  $u$ , and  $V$  are assumed to be functions of  $x$ , whereas from the equation of continuity it follows that  $J$  is independent of  $x$ . The charge density  $\rho$  is negative, and  $u$  is positive. Eliminating  $\rho$  and  $u$  from the above equations, we obtain

$$\frac{d^2V}{dx^2} = \frac{J}{\epsilon_0\sqrt{2(e/m)V}} \quad (4.1-5)$$

Next, both sides of this equation can be multiplied by  $dV/dx$  and integrated with respect to  $x$  from  $x = 0$  to  $x$ , giving

$$\left| \frac{dV}{dx} \right|^2 = \frac{4J V^{1/2}}{\epsilon_0\sqrt{2(e/m)}} + C_1 \quad (4.1-6)$$

Since  $V = dV/dx = 0$  at  $x = 0$ , the constant  $C_1$  is zero. Taking the square root of both sides and integrating once more, we obtain

$$(4/3)V^{3/4} = 2\sqrt{J/\varepsilon_0}(m/2e)^{1/4}x + C_2 \quad (4.1-7)$$

Since  $V = 0$  at  $x = 0$ ,  $C_2$  is also zero. Finally, this equation can be solved for the current density  $J$ , giving

$$J = \frac{4}{9\varepsilon_0}\sqrt{2(e/m)}\frac{V^{3/2}}{x^2} \quad (4.1-8)$$

If the experimental values of  $e$ ,  $m$ , and  $\varepsilon_0$  are substituted in this expression, it becomes

$$J = 2.33 \times 10^{-6}\frac{V^{3/2}}{x^2} \text{ amps/meter}^2 \quad (4.1-9)$$

Here  $V = V(x)$  is the potential at a point  $x$  meters from the virtual cathode. If the applied anode voltage is  $V_{ao}$  volts above that of the potential minimum, and if the distance from the virtual cathode to the anode is  $d$  meters, the current density is given by

$$J = 2.33 \times 10^{-6}\frac{V_{ao}^{3/2}}{d^2} \text{ amps/meter}^2 \quad (4.1-10)$$

If  $V_{ao} \gg V_m$ , the voltage  $V_{ao}$  can be taken to be the anode-to-cathode voltage. Similarly, the distance from the cathode to the potential minimum is usually small compared with the distance from the potential minimum to the anode, so that  $d$  can be taken to be the anode-to-cathode distance. Hence, to a good approximation, the current drawn from the cathode under space-charge-limited conditions varies as the 3/2 power of the anode voltage divided by the square of the anode-to-cathode distance. This result is known as the Child-Langmuir Law. Langmuir<sup>2</sup> also developed more accurate equations for the planar diode which take into account the distribution of electron emission velocities and which show the location of the potential minimum. However, for most purposes, Equation (4.1-10) gives a sufficiently accurate expression for the current density  $J$ , and the potential minimum can be assumed to be very close to the cathode.

## 4.2 Diodes with Other Electrode Geometries

Two further conclusions concerning Equations (4.1-9) and (4.1-10) are of interest:

1. If  $A$  is the cathode area of a planar diode, the current drawn to the anode under space-charge-limited conditions is given by  $JA = 2.33 \times 10^{-6} V_{ao}^{3/2} A/d^2$ . Because of the factor  $A/d^2$  in this expression, it is evident that,

<sup>2</sup>Reference 4.1.

if the linear dimensions of a planar diode are increased by a factor  $k$ , the same current flows to the anode for the same applied voltage.

2. Combining Equations (4.1-9) and (4.1-10), we obtain

$$V(x) = \frac{x^{4/3}}{d^{4/3}} V_{a0} \quad (4.2-1)$$

Hence, despite the fact that increasing the anode voltage increases the current drawn from the cathode, the potential at points between the electrodes remains directly proportional to the applied anode voltage.

Equations describing the space-charge-limited flow of electrons between concentric cylinders and concentric spheres have also been derived.<sup>3</sup> In each of these cases, it is found that: (1) The current drawn to the anode is proportional to the 3/2 power of the applied anode voltage; (2) if two diodes differ by a factor  $k$  in their linear dimensions, the same current flows to the anode when the same anode voltage is applied; and (3) the potential

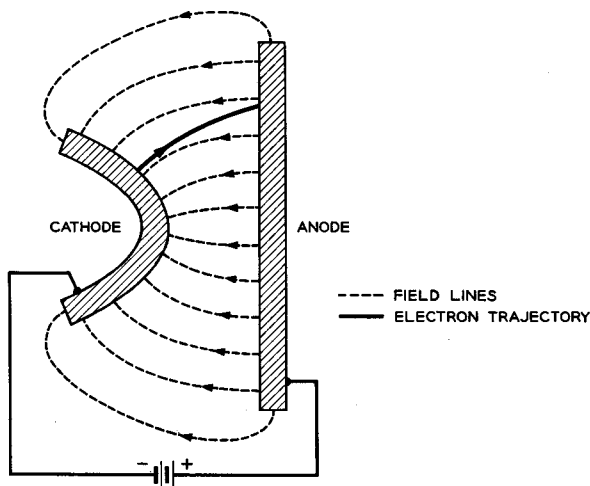


Fig. 4.2-1 A diode with a parabolic-shaped cathode and a planar anode.

at points between the electrodes is directly proportional to the applied anode voltage when space-charge-limited conditions apply.

In the planar, cylindrical, and spherical diodes, the field lines are straight, and the electron trajectories are parallel to the field lines. However, in diodes with other electrode geometries, this is not the case; when the field lines are curved, the electron trajectories cross the field lines. This effect is

<sup>3</sup>Reference 4.1, p. 245, and References 4.2 and 4.3.



illustrated in Figure 4.2-1 for a diode consisting of a parabolic-shaped cathode and a planar anode. The trajectory of a single electron is shown in the figure. Because the electron has inertia, the path it follows does not bend as sharply as the field lines.

The question then arises as to whether in a space-charge-limited diode with arbitrarily shaped electrodes the electron trajectories change their shape when the anode voltage is varied. To answer this question, suppose that  $V = V_1(x, y, z)$  and  $\rho = \rho_1(x, y, z)$  are steady-state solutions for the potential and charge in the interelectrode space of a particular diode. These solutions meet the following boundary conditions:  $V = V_{a0}$  at the anode surface,  $V = dV/dn = 0$  at the potential minimum (which we shall assume coincides with the cathode surface). Here  $d/dn$  is the derivative in the direction normal to the cathode surface. From Poisson's equation it follows that, if the anode voltage is now changed to  $kV_{a0}$ , solutions of the potential and charge distribution which meet the new boundary conditions are given by  $V = kV_1(x, y, z)$  and  $\rho = k\rho_1(x, y, z)$ . Furthermore, it is shown in Appendix VII that only one steady-state solution of Poisson's Equation will meet the boundary conditions for a space-charge-limited diode. It follows, therefore, that the potential in the interelectrode space of a space-charge-limited diode with arbitrarily shaped electrodes is directly proportional to the applied anode voltage. This being the case, we can invoke the same arguments that were used in Section 1.1 to show that the electron trajectories are not affected by changes in positive anode voltage. This conclusion, in fact, is experimentally verified, apart from effects arising from the finite emission velocity of the electrons.

Next let us consider how the current density  $J = -\rho u$  in the interelectrode space of a diode with arbitrarily shaped electrodes varies with the applied anode voltage when space-charge-limited conditions prevail. From the relationship,

$$\frac{1}{2}mu^2 = eV(x, y, z) \quad (4.2-2)$$

we see that  $u = u(x, y, z)$  is proportional to the square root of  $V(x, y, z)$ , and hence it is proportional to the square root of the applied anode voltage. The charge density  $\rho = \rho(x, y, z)$  is related to the potential  $V(x, y, z)$  by

$$\nabla^2 V(x, y, z) = -\frac{\rho}{\epsilon_0} \quad (4.2-3)$$

Since  $V(x, y, z)$  is proportional to the applied anode voltage, and since the Laplacian operator is linear, it follows that  $\rho$  is directly proportional to the applied anode voltage. Consequently,  $J = -\rho u$  is proportional to the 3/2 power of the applied anode voltage. Thus the current drawn to the anode

of a space-charge-limited diode having arbitrarily shaped electrodes is proportional to the  $3/2$  power of the applied anode voltage.

By similar reasoning we can deduce that, if the dimensions of a diode with arbitrarily shaped electrodes are scaled by a constant factor and if the tube is operated under space-charge-limited conditions, the total current drawn to the anode for a given applied anode voltage is unchanged. Let us suppose that the linear dimensions of a diode are increased by the factor  $k$ . The potential at corresponding points between the electrodes remains the same for the same applied anode voltage, so that the electron velocity  $u$  at corresponding points between the electrodes remains the same. However,  $\partial V/\partial x$  is changed by  $1/k$ , and  $\partial^2 V/\partial x^2$  is changed by  $1/k^2$ . Since  $\rho$  is proportional to  $\nabla^2 V(x,y,z)$ , it follows that  $\rho$  is changed by  $1/k^2$ . Consequently, the current density  $J = -\rho u$  is changed by  $1/k^2$ ; and since the electrode area is  $k^2$  times its previous value, the current drawn to the anode for the same applied anode voltage remains unchanged.

### 4.3 Two Examples of Diode Rectifiers

#### *The 412A*

Figure 4.3-1 shows the construction of the Western Electric 412A full-wave diode rectifier. The tube consists of two diodes with indirectly

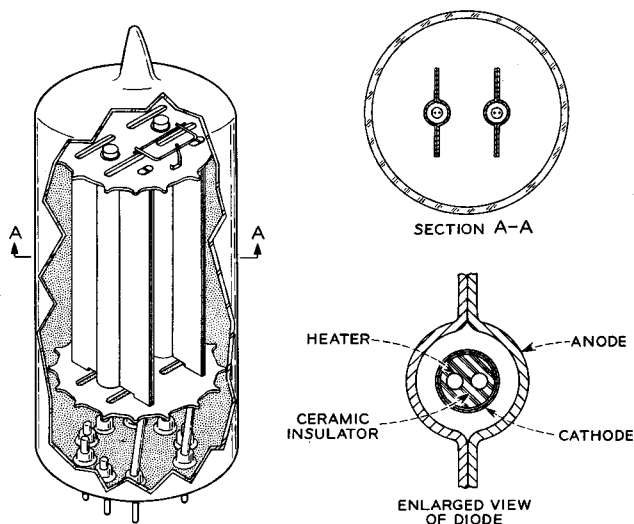


FIG. 4.3-1 The construction of the Western Electric 412A full-wave diode rectifier. The overall height of the tube is 6.7 cm.

heated cathodes enclosed in a common envelope. A ceramic insulator separates the heater of each diode from the cathode. The cathodes are cylindrical sleeves of nickel with a "double-carbonate" oxide coating on the outer side. The cathode-anode spacing is 0.5 mm. The anodes are made of nickel which is coated with fine carbon particles in order to increase the heat radiation from the outer surface. This in turn enables the anodes to operate at a lower temperature for a given power dissipation.

Figure 4.3-2 shows measurements of anode current vs. anode voltage for the 412A for several heater voltages. The normal heater operating voltage

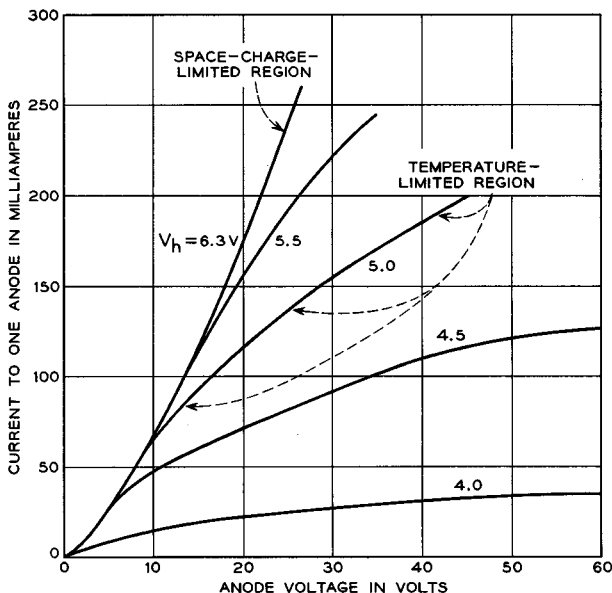


FIG. 4.3-2 Anode current vs. anode voltage for the 412A for several heater operating voltages  $V_h$ . The normal heater operating voltage is 6.3 volts.

is 6.3 volts. At  $V_h = 6.3$  volts, the anode current is space-charge-limited over the range of anode voltages for which the data are plotted, and the anode current increases very nearly as the  $3/2$  power of the anode voltage. At the other filament voltages for which data are plotted in the figure, the anode current is space-charge-limited at lower anode voltages and "temperature-limited" at higher anode voltages. In the region of "temperature-limited" operation, the anode current actually increases with increasing anode voltage rather than remaining constant, as it would in an ideally temperature-limited diode. It is thought that this can be attributed to

the rough and porous nature of the oxide-cathode emitting surface. At the onset of temperature-limited operation only the current drawn from the outermost parts of the cathode surface is temperature-limited, whereas the current drawn from the re-entrant parts and the entrances to the pores is still space-charge-limited. Thus, with increasing anode voltage, the current drawn from regions that are still space-charge-limited continues to increase, but the total area from which space-charge-limited current is drawn decreases. Operation of the tube for an extended time in the temperature-limited region is found to be harmful to cathode life.

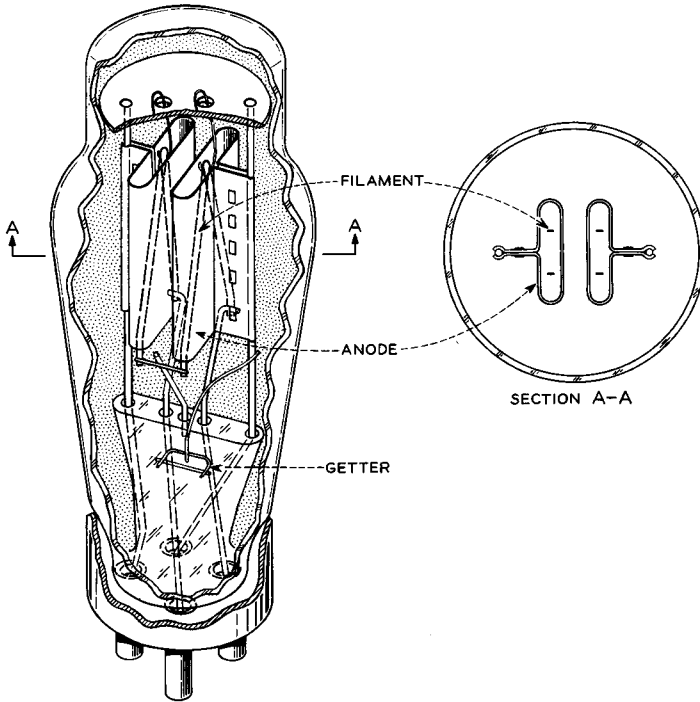


FIG. 4.3-3 The construction of the Western Electric 274B full-wave diode rectifier. The over-all height of the tube is 13.8 cm.

Maximum ratings for the 412A are given in Table 4.3-1. The use of a ceramic insulator between the heater and cathode permits operation of the diodes with as much as 450 volts potential difference between the heater and cathode.

TABLE 4.3-1

	<i>Maximum Rating</i>
Peak inverse voltage*, volts . . . . .	1250
Peak anode current per anode, ma . . . . .	300
DC output current (when operated as a full-wave rectifier), ma . . . . .	100
DC heater-cathode potential, volts . . . . .	450

\*Maximum negative voltage applied to the anode with respect to cathode voltage.

**The 274B**

The construction of the Western Electric 274B full-wave diode rectifier is illustrated in Figure 4.3-3. The tube consists of two diodes with filamentary cathodes enclosed in a common envelope. The filaments are made from a nickel alloy and have a “double-carbonate” oxide coating. The nickel alloy contains the following elements in addition to nickel:

<i>Element</i>	<i>Per Cent by Weight</i>	<i>Element</i>	<i>Per Cent by Weight</i>
Co . . . . .	0.5 to 0.75	C . . . . .	0.04 to 0.07
Cu . . . . .	< 0.10	Si . . . . .	< 0.03
Fe . . . . .	< 0.15	Mg . . . . .	0.04 to 0.08
Mn . . . . .	< 0.20	Ti . . . . .	< 0.03

These small amounts of impurities in the nickel increase its resistivity and mechanical strength. The elements in the right-hand half of the table

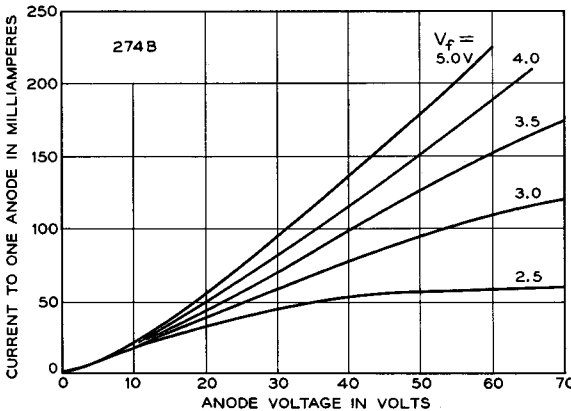


FIG. 4.3-4 Anode current vs. anode voltage for the 274B for several filament operating voltages  $V_f$ . The normal filament operating voltage is 5.0 volts.

also serve as the reducing agents which maintain the activity of the oxide coating. The filaments are connected in series within the envelope of the tube. The anodes are made of carbonized nickel, as in the 412A.

Figure 4.3-4 shows measurements of the anode current vs. anode voltage for the 274B. The normal filament operating voltage is 5.0 volts. The shape of the curves in the "temperature-limited" region is further complicated for this tube by the facts that the distance from the filament surface to the anode varies over the filament surface and that there is a voltage drop along the length of the filament. Consequently, the onset of temperature-limited operation occurs at different anode voltages for different parts of the filament surface.

Maximum ratings for the tube are given in Table 4.3-2.

TABLE 4.3-2

	<i>Maximum Rating</i>
Peak inverse voltage, volts . . . . .	1500
Peak anode current per anode, ma . . . . .	675
DC output current (when operated as a full-wave rectifier), ma . . .	225

#### 4.4 Some Effects of Thermal Emission Velocities

Appendix IV summarizes the relations pertaining to the velocity distribution, energy distribution, and angular distribution of the electrons emitted from a thermionic cathode, as discussed in Section 2.4.

Because the electrons are emitted with a finite component of velocity parallel to the cathode surface, they tend to drift across the beam while being drawn away from the cathode by the applied field. In consequence of this, the electron beams generated by electron guns are always larger than they would be if the electron emission velocity were zero.

As a simple example to illustrate the sideways drift of electrons in an accelerating field, let us consider the electron trajectories in the planar, parallel diode shown in Figure 4.4-1. (In the illustrations used in this section, it will be convenient to identify the trajectories of electrons emitted from the cathode with zero kinetic energy with solid lines, and the trajectories of electrons having finite kinetic energy at the time of emission with broken lines. The former electrons will be called *nonthermal* electrons, and the latter will be called *thermal* electrons.) Suppose the anode-to-cathode spacing of the diode shown in Figure 4.4-1 is 1 cm, and a voltage of +10 volts is applied to the anode. We shall assume that the cathode emission is very small and temperature-limited and that the electric field between the electrodes is uniform. Consider an electron which is emitted from the cathode with 1/10 electron volt of kinetic energy parallel to the

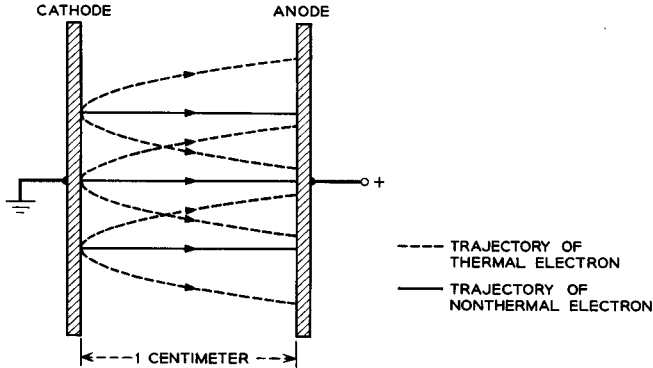


FIG. 4.4-1 Some electron trajectories in the interelectrode space of a planar diode.

cathode surface and no kinetic energy normal to the surface. At the time the electron strikes the anode, the ratio of its transverse energy to its energy in the direction of the accelerating field is  $1/100$ . The corresponding ratio of velocities is equal to the square root of this, or  $1/10$ . Since the final velocity in the direction of the accelerating field is twice the average velocity, the ratio of the transverse velocity of the electron to its average velocity in the direction of the field is  $2/10$ . Consequently, the electron does not strike the anode at a point directly opposite its point of emission, but 2 millimeters to one side.

If the cathode temperature in the above example were  $1160^\circ\text{K}$ , the electron we have considered would have had average transverse energy, since  $W_T = T/11,600$  electron volts is the average transverse energy. Other electrons would be emitted with appreciably greater transverse energies. Furthermore, if the current drawn from the cathode were space-charge-limited, the time taken by an electron to reach the anode would be at least  $3/2$  as great (Problem 4.1), so that the electrons would drift even farther to the side. Of course, by increasing the accelerating voltage, the amount of sideways drift is reduced. If the anode voltage in the above example were increased to 1000 volts, the electron would drift only 0.2 mm to the side for the case of the uniform accelerating field.

Let us now consider the distribution of points of arrival on the anode of electrons emitted from a single point on the cathode of a planar diode. Suppose an electron emitted from a point on the cathode with transverse velocity  $\sqrt{kT/m}$  drifts a distance  $\sigma$  to the side in traveling from the cathode to the anode. If the anode voltage is large compared with  $kT/e$ , we can neglect the effects of emission velocities normal to the cathode (to a first approximation) and assume a constant time for electrons to travel from the cathode to the anode. In this case, an electron emitted from the cathode

with transverse velocity  $u_t$ , would drift a distance  $r$  to the side while traveling from the cathode to the anode, where

$$r = \frac{u_t}{\sqrt{kT/m}}\sigma \quad (4.4-1)$$

Rearranging this equation, we obtain

$$u_t = \frac{r}{\sigma}\sqrt{kT/m} \quad (4.4-2)$$

Substituting for  $u_t$  in Equation (2) of Appendix IV from the above equation, we find that the probability that an electron, which is incident upon the anode, is displaced a distance in the range  $r$  to  $r + dr$  from the point on the anode directly opposite its point of emission is given by

$$dP(r) = \frac{1}{2\sigma^2}e^{-r^2/2\sigma^2}dr^2 \quad (4.4-3)$$

Equation (4.4-3) implies a Gaussian distribution in two dimensions, and  $\sigma$  can be identified as the standard deviation of the distribution. Thus electrons emitted from a single point on the cathode will be incident upon the anode at points whose density is given by a two-dimensional Gaussian function with standard deviation  $\sigma$ .

An electron emitted from the cathode of a planar diode with a component of velocity parallel to the cathode follows a curved trajectory which bends increasingly toward the normal to the electrodes. For this reason, the current density of electrons arriving at the anode per unit solid angle in the direction normal to the anode is far higher than the cathode emission current density per unit solid angle in the direction normal to the cathode. From Equation (7) of Appendix IV it follows that the latter quantity is  $J_o/\pi$ , where  $J_o$  is the total cathode emission current density. Let us proceed now to obtain the current density of electrons arriving at the anode per unit solid angle in the direction normal to the anode. We shall use this quantity in later discussion.

We shall assume, as before, that fringing fields at the edge of the diode can be neglected, and that an electron emitted from the cathode with a component of velocity in the direction parallel to the cathode will maintain this component of velocity throughout its travel from the cathode to the anode. In this case, an electron which is emitted from the cathode in a direction making an angle  $\theta_1$  with the normal to the cathode, and which has kinetic energy  $eV_1$  joules at the time of emission, will be incident upon the anode at an angle  $\theta_2$  with respect to the normal such that

$$\sin\theta_2 = \frac{V_1^{1/2}}{(V_1 + V_2)^{1/2}}\sin\theta_1 \quad (4.4-4)$$



where  $V_2$  is the cathode-anode potential difference. Differentiating both sides of this gives

$$\cos\theta_2 d\theta_2 = \frac{V_1^{1/2}}{(V_1 + V_2)^{1/2}} \cos\theta_1 d\theta_1 \quad (4.4-5)$$

From Equations (5) and (6) of Appendix IV, the current density of electrons emitted from the cathode with kinetic energy between  $eV_1$  and  $e(V_1 + dV_1)$  joules and with emission velocities lying in the angular range  $\theta_1$  to  $\theta_1 + d\theta_1$  with respect to the normal is

$$dJ(V_1, \theta_1) = J_o \frac{eV_1}{kT} \epsilon^{-eV_1/kT} \frac{deV_1}{kT} 2 \sin\theta_1 \cos\theta_1 d\theta_1 \quad (4.4-6)$$

where  $J_o$  is the total cathode emission current density. This is also the current density at the anode due to electrons which are emitted from the cathode with kinetic energy in the range  $eV_1$  to  $e(V_1 + dV_1)$  joules, and which arrive at the anode with angles of incidence in the range  $\theta_2$  to  $\theta_2 + d\theta_2$ , where  $\theta_2$  is related to  $\theta_1$  by Equation (4.4-4). Thus the current density arriving at the anode per unit solid angle at an angle  $\theta_2$  with respect to the normal, and which is composed of electrons emitted from the cathode with kinetic energy in the range  $eV_1$  to  $e(V_1 + dV_1)$  joules, is

$$\frac{dJ(V_1, \theta_1)}{2\pi \sin\theta_2 d\theta_2} = \frac{J_o e(V_1 + V_2)}{\pi kT} \epsilon^{-eV_1/kT} \frac{deV_1}{kT} \cos\theta_2 \quad (4.4-7)$$

where we have substituted from Equations (4.4-4) and (4.4-5) for  $\sin\theta_1$  and  $\cos\theta_1 d\theta_1$ . By setting  $\cos\theta_2 = 1$  in the right-hand side of Equation (4.4-7), we obtain the current density which arrives at the anode per unit solid angle in the direction *normal* to the anode and which is composed of electrons emitted from the cathode with kinetic energy in the range  $eV_1$  to  $e(V_1 + dV_1)$ . Then, by integrating this quantity with respect to  $V_1$  from zero to infinity, the total current density incident upon the anode per unit solid angle in the direction normal to the anode is found to be

$$J_a(\theta_2 = 0) = \frac{J_o}{\pi} \left( \frac{eV_2}{kT} + 1 \right) \quad (4.4-8)$$

This is the expression we set out to derive. It compares with a cathode emission current density per unit solid angle in the direction normal to the cathode of  $J_o/\pi$ . In the discussion that follows we shall use Equation (4.4-8) to obtain an approximate expression for the maximum current density which can be obtained at a crossover.

Figure 4.4-2 shows a planar diode in which the anode has a small circular aperture. Two additional electrodes located behind the anode combine with the anode to form an einzel lens. (See Figures 3.1-1(c) and 3.1-1(d).) The beam of electrons passing through the lens is focused to a crossover  $L$

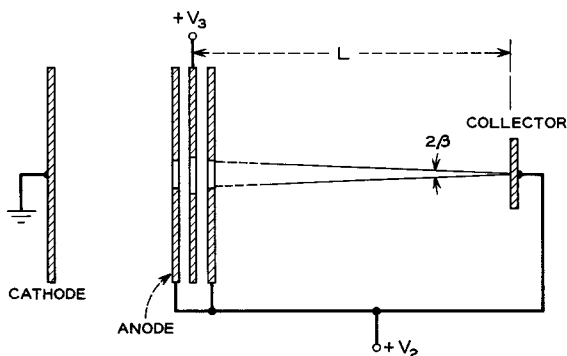


FIG. 4.4-2 A planar diode with a small circular aperture in the anode. Two apertured electrodes behind the anode combine with the anode to form an einzel lens. The electrons passing through the anode aperture are focused to a crossover at the collector electrode.

units from the lens. A collector electrode at the crossover intercepts the beam. Let us now estimate the current density at the center of the crossover. We shall assume that Equation (4.4-8) gives the current density incident upon the anode aperture per unit solid angle in the direction normal to the aperture. We shall further assume that electrons emitted from the cathode with zero transverse velocity and incident upon the anode aperture from the cathode side are deflected by the lens in the direction of the center of the crossover. An element of area  $dA$  in the center of the crossover and normal to the beam axis will subtend a solid angle  $dA/L^2$  at a point on the aperture. Therefore, unit area of the aperture will transmit a current  $\frac{J_o(eV_2}{\pi(kT} + 1) \frac{dA}{L^2}$  to the element of area  $dA$ , and the current density incident upon  $dA$  from unit area of the aperture will be  $\frac{J_o(eV_2}{\pi(kT} + 1) \frac{1}{L^2}$ . If the radius of the aperture is  $R$ , the total current density at the center of the crossover will be

$$J_o \left( \frac{eV_2}{kT} + 1 \right) \frac{R^2}{L^2} \quad (4.4-9)$$

More accurately, it can be shown with the aid of statistical mechanics<sup>4</sup> that the maximum current density obtainable at a crossover with *any* lens system is given by

$$J_o \left( \frac{eV_2}{kT} + 1 \right) \sin^2 \beta \quad (4.4-10)$$

<sup>4</sup>Reference 4.4. See also Reference 4.5.

where  $\beta$  is the half angle subtended at the crossover by the aperture diameter. Moreover, it can be shown that this limiting current density can be approached only when the aperture of the lens system passes a small part of the total current drawn from the cathode, and when the lens system is essentially aberration-free. The limiting current density given by the above expression applies both at a crossover and at an image of a crossover formed by a subsequent lens system.

In a cathode-ray tube the half angle  $\beta$  of the cone of trajectories incident upon the screen is often of the order of 1/100 radian or smaller, whereas  $eV_2$  may be  $5 \times 10^4$  times  $kT$ . Thus the maximum current density obtainable at the screen of the tube is often of the same order of magnitude as the cathode current density  $J_0$ . However, because of aberrations, the actual current density at the screen is usually less than  $J_0$ .

Suppose that in the device shown in Figure 4.4-2 an electron emitted from the cathode with transverse velocity  $\sqrt{kT/m}$  passes through the anode aperture and strikes the collector at a point  $\sigma$  units from the center of the crossover. If we assume that the transit time from the cathode to the collector is the same for all electrons reaching the collector and that aberrations in the einzel lens are small, an electron that leaves the cathode with transverse velocity  $u_t$  will be displaced a distance  $r = u_t \sigma / \sqrt{kT/m}$  from the beam axis by the time it reaches the crossover. We then can use the same arguments that were presented in connection with Equation (4.4-3) to show that the current density incident upon the collector is proportional to

$$\epsilon^{-r^2/2\sigma^2} d \frac{r^2}{2\sigma^2}$$

where  $r$  is the distance measured along the surface of the collector from the beam axis.

If the lens in Figure 4.4-2 is made stronger,  $L$  decreases and  $\beta$  increases. However,  $\sigma$  decreases, since the transit time from the aperture to the crossover is smaller. Similarly, decreasing the strength of the lens reduces  $\beta$  and increases  $\sigma$ . (Ultimately the beam will diverge at the lens.) Thus an electron beam can be focused to a crossover of small diameter and large angle of convergence  $\beta$ , or a large diameter and small angle of convergence, but not simultaneously to a small diameter and small angle of convergence.

Next let us consider some effects of thermal emission velocities in convergent beams such as are used in many microwave tubes. Figure 4.4-3 shows a diode with a cathode emitting surface and anode which are portions of spheres, both concentric about the point  $P$ . Nonthermal electrons in such a diode travel in radial lines from the cathode to the anode, since the forces acting on them are directed toward the point  $P$ . The trajectory of one thermal electron is shown in the figure. Suppose this electron is emitted

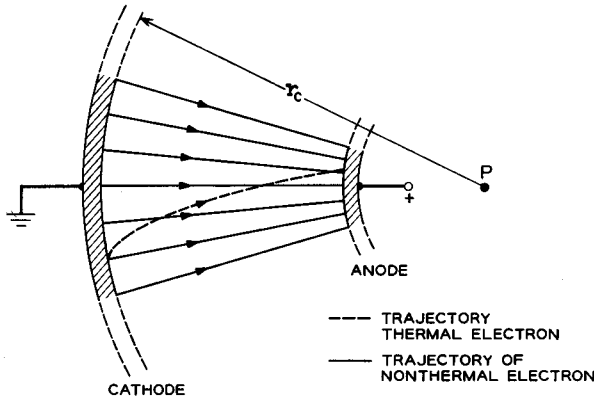


FIG. 4.4-3 Trajectories of a thermal electron and several nonthermal electrons in a spherical diode.

with velocity  $u_{ic}$  parallel to the cathode surface. Since the forces acting on it are directed toward the point  $P$ , angular momentum about the point  $P$  is conserved. When the electron reaches radius  $\bar{r}$  from the point  $P$ , its component of velocity  $u_{tr}$  transverse to the radial direction is given by

$$m u_{tr} \bar{r} = m u_{ic} \bar{r}_c \quad (4.4-11)$$

or

$$u_{tr} = \frac{\bar{r}_c}{\bar{r}} u_{ic} \approx \frac{d_c}{d} u_{ic} \quad (4.4-12)$$

where  $\bar{r}_c$  is the radius of the cathode emitting surface measured from the point  $P$  to the cathode emitting surface,  $d_c$  is the cathode diameter, and  $d$  is the diameter of the beam at radius  $\bar{r}$  from point  $P$ . Consequently, as the thermal electron travels from the cathode toward the anode, its component of velocity transverse to the nonthermal electron trajectories increases, and at a given point it is inversely proportional to the beam diameter at that point. This result applies when the current drawn from the cathode is space-charge-limited as well as when it is temperature-limited.

The foregoing is a particular example of a quite general relationship which applies to paraxial electron beams. This relationship states that, if the diameter of an electron beam is reduced from  $d_1$  to  $d_2$  by the action of axially symmetric fields and if the fields acting on the electrons are directly proportional to the distance from the beam axis, the transverse velocities of the thermal electrons measured relative to the trajectories of the nonthermal electrons are increased by the ratio  $d_1/d_2$ . The discussion presented below will develop this more general relationship.

It will be convenient to introduce a radial coordinate  $\mu$  which varies linearly from zero on the beam axis to unity at the beam edge. Let  $r_e(z)$  be the beam radius (corresponding to  $\mu = 1$ ). We shall assume that the non-thermal electrons travel in laminar paths, that is, paths that do not cross one another, and that the radial forces within the beam are directly proportional to distance from the axis. The path traveled by a nonthermal electron is therefore one of constant  $\mu$ . If there is appreciable space charge in the beam, the assumption that the radial forces are proportional to distance from the axis implies a uniform current density over the beam cross section. (See Equation (3.4-9).)

Consider a thermal electron whose radial coordinate is given by

$$r = \mu r_e \quad (4.4-13)$$

where both  $\mu$  and  $r_e$  are functions of  $z$ . Differentiating this equation twice with respect to time gives

$$\dot{r} = \dot{\mu} r_e + 2\mu \dot{r}_e + \mu \ddot{r}_e \quad (4.4-14)$$

where

$$\dot{r}_e = r_e' \dot{z} \quad (4.4-15)$$

and

$$\ddot{r}_e = r_e''(\dot{z})^2 + r_e' \ddot{z} \quad (4.4-16)$$

Similar expressions hold for  $\dot{\mu}$  and  $\ddot{\mu}$ . (The notation used here is similar to that of Chapter 3.) Since the radial forces acting on the thermal electron are directly proportional to its distance from the axis, the radial acceleration of the thermal electron is  $\mu$  times the radial acceleration of a non-thermal electron at the edge of the beam, or

$$\ddot{r} = \mu \ddot{r}_e \quad (4.4-17)$$

Comparing this equation with Equation (4.4-14), we see that

$$\dot{\mu} r_e + 2\mu \dot{r}_e = 0 \quad (4.4-18)$$

or

$$\frac{d}{dt}(\dot{\mu} r_e^2) = 0 \quad (4.4-19)$$

Integrating this, we find that

$$\dot{\mu} r_e^2 = \text{constant} \quad (4.4-20)$$

a relationship which applies over the whole length of the beam. Consider two points on the electron's trajectory such that  $\mu = \mu_1$  at one point and

$\mu = \mu_2$  at the second point. Let the beam radius be  $r_{e1}$  at the first point and  $r_{e2}$  at the second point. Then, from Equation (4.4-20),

$$\frac{\dot{\mu}_2 r_{e2}}{\dot{\mu}_1 r_{e1}} = \frac{r_{e1}}{r_{e2}} \quad (4.4-21)$$

Now the quantity  $\dot{\mu}_1 r_{e1}$  is the transverse velocity of the thermal electron measured relative to the trajectories of the nonthermal electrons at the point where the beam radius is  $r_{e1}$ . We shall denote it by  $u_{t1}$ . Similarly we shall set  $u_{t2} = \dot{\mu}_2 r_{e2}$ . Equation (4.4-21) therefore can be written as

$$u_{t2} = \frac{r_{e1}}{r_{e2}} u_{t1} = \frac{d_1}{d_2} u_{t1} \quad (4.4-22)$$

where  $d_1 = 2r_{e1}$ , and  $d_2 = 2r_{e2}$ . This is the relation we set out to obtain.

The case we have just considered applied to a thermal electron whose initial transverse velocity is in the *radial* direction only. If the thermal electron also has an initial component of velocity in the  $\theta$  direction, that is, the direction both perpendicular to the beam axis and the radial direction, we can use a Cartesian coordinate system in the transverse plane to describe the transverse motion of the electron. For an axially symmetric electric field in which  $E_r = ar$ , the  $x$  and  $y$  components of the radial field can be expressed as  $E_x = ax$  and  $E_y = ay$ . Furthermore we can rewrite the foregoing equations replacing  $r$  by  $x$  or  $y$  and  $\mu$  by  $\mu_x$  or  $\mu_y$ . In this way it is easily shown that Equation (4.4-22) applies for any direction of the initial transverse velocity  $u_{t1}$ .

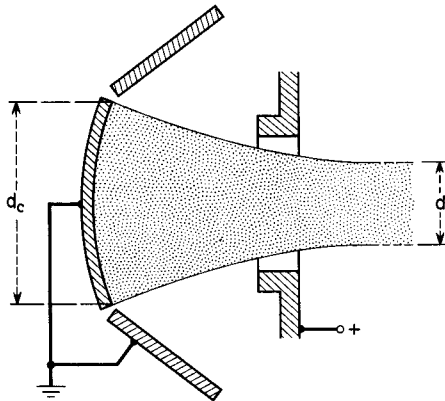


FIG. 4.4-4 A convergent electron gun which generates a beam of diameter  $d$  from a cathode of diameter  $d_c$ .

The foregoing results can be applied to an electron gun which generates a beam of diameter  $d$  and has a cathode of diameter  $d_c$ . Such a gun is illustrated in Figure 4.4-4. The average transverse velocity of the electrons in the region where the beam diameter is  $d$  will be  $d_c/d$  times the average transverse velocity at the cathode surface, and from Equation (2) of Appendix IV the probability that an individual electron has transverse velocity in the range  $u_t$  to  $u_t + du_t$  at a point where the beam diameter is  $d$  will be

$$dP(u_t) = \frac{m u_t}{kT} \left( \frac{d}{d_c} \right)^2 \epsilon^{-m u_t^2 (d/d_c)^2 / 2kT} du_t \quad (4.4-23)$$

Highly convergent electron guns (guns with high  $d_c/d$ ) therefore generate electron beams with high transverse velocities.

## 4.5 Electron Guns

It will be convenient to consider separately the electron guns used in microwave tubes and those used in cathode-ray tubes and storage tubes, since the principles involved in the two cases are quite different.

### a. Electron Guns Used in Microwave Tubes

Figure 4.5-1 shows three electron guns that are used in beam-type microwave tubes. The first two have a relatively large cathode area in order to draw the required total emission current, and electrodes in front of the cathode focus the beam to a cross section much smaller than the cathode area. In this way electron beams of current density far greater than the cathode emission density can be obtained. The third electron gun is operated in a uniform axial magnetic field, so that the electron beam cross section is just a little larger than the cathode area, and the electron motion

TABLE 4.5-1

Gun	a	b	c
Beam voltage, volts.....	2600	500	570
Beam current, amp.....	0.040	0.066	0.0005
Perveance, amp/volts <sup>3/2</sup> .....	$0.30 \times 10^{-6}$	$5.9 \times 10^{-6}$	$3.7 \times 10^{-8}$
Cathode current density, amp/cm <sup>2</sup> .....	0.21	0.19	0.16
Average beam current density, amp/cm <sup>2</sup> ..	5	7	~ 0.1
Angle of convergence*, degrees.....	25	145	—

\*The angle subtended by a diameter of the cathode at the center of curvature of the cathode emitting surface.

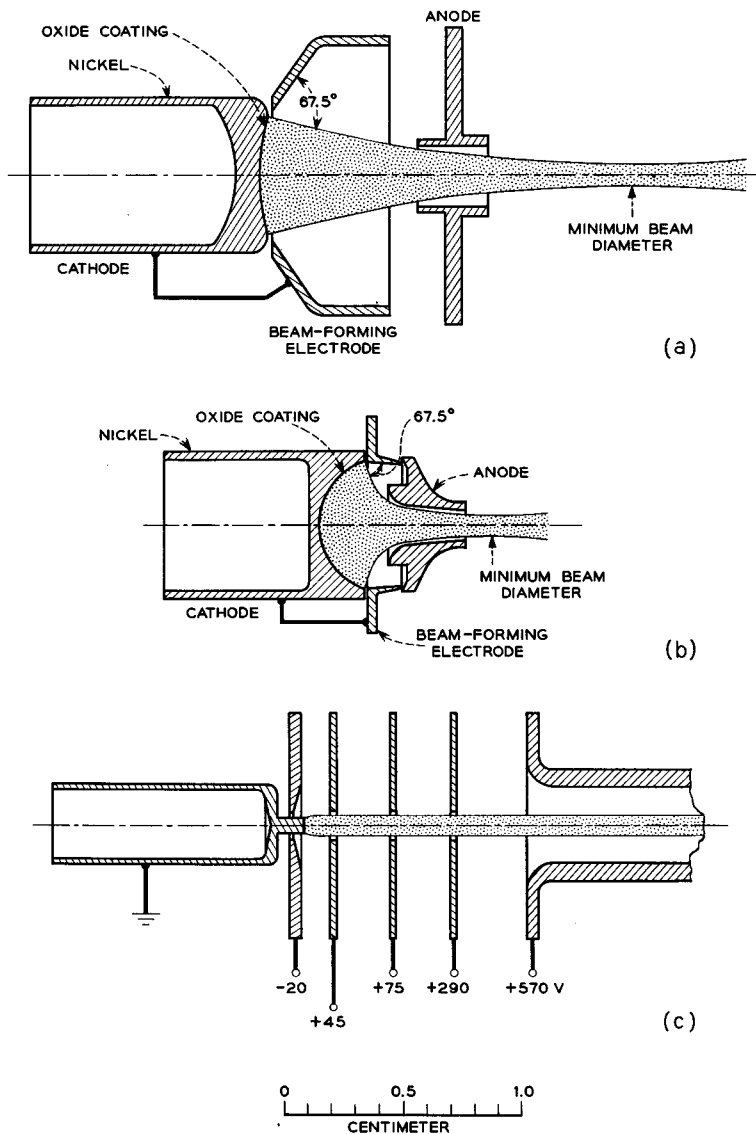


FIG. 4.5-1 Three electron guns used in microwave tubes.

is similar to that described in Section 3.4(b) under the heading of Confined Flow. Table 4.5-1 lists several important characteristics of these guns.

The electron gun shown in Figure 4.5-1(a) consists of a cathode, a "beam-



forming electrode," which is operated at cathode potential, and an anode. The cathode emitting surface is concave and spherical in shape. The gun is called a Pierce electron gun, after J. R. Pierce,<sup>5</sup> who first put the design of convergent electron guns on a firm basis.

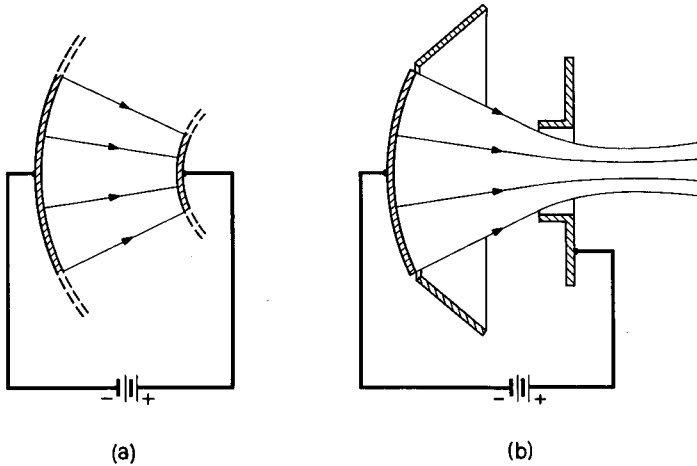


FIG. 4.5-2 The evolution of a Pierce electron gun from a spherical diode.

To understand the choice of shape for the electrodes, we might first imagine a diode consisting of portions of two concentric spheres, such as the one illustrated in Figure 4.5-2(a). The cathode and anode are assumed to be defined by the intersection between the spherical surfaces and a right-circular cone with apex at the common center of the spheres. With such a device we can make a convergent beam of electrons. However, the nonthermal edge electrons travel in radial lines only if they experience a radial electric field and no transverse field. A little consideration shows that this will be the case only if the potential just outside the beam varies with radius  $\bar{r}$  (measured from the common center of the spheres) in the same way that it does inside the beam. The beam-forming electrode, therefore, is designed to create a potential along the edge of the beam which matches as nearly as possible that inside the beam. Finally, since we do not want to intercept the electrons, a hole must be made in the anode so that the convergent beam will pass on through. The resulting shape of the electron gun is similar to that shown in Figure 4.5-2(b).

The beam-forming electrode has its principal effect close to the cathode, where the electrons are moving more slowly and the transverse fields are

<sup>5</sup>Reference 4.6.

able to deflect the electron trajectories much more. Let us examine the shape of the beam-forming electrode in this region more closely. Figure 4.5-3 shows a much expanded view of the edge of the beam close to the

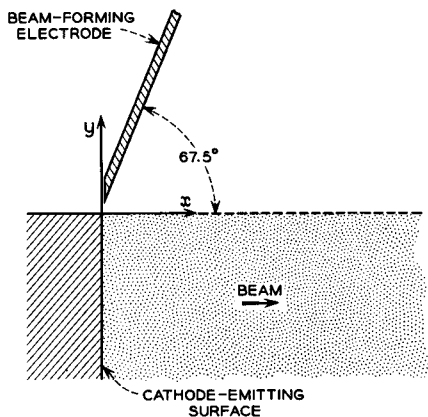


FIG. 4.5-3 An expanded view of the edge of the beam in the region of the cathode.

cathode emitting surface. If the dimensions of the portion of the cathode shown in the figure are assumed to be small compared with the overall cathode dimensions, we can further assume that the portion of the emitting surface shown in the figure is *planar* and that the beam extends a considerable distance above and below the page. The potential problem then reduces to a *two-dimensional* one and is thereby simplified. In the portion of the beam we are considering, the potential will vary approximately as in the planar diode and will be given by

$$V = Ax^{4/3} \quad (4.5-1)$$

where  $A$  is a constant, and  $x$  is the distance measured from the emitting surface.

Appendix VIII considers two-dimensional potentials which are symmetric about an axis. It is shown there that, if the  $x$  axis of a Cartesian coordinate system is the axis of symmetry and if  $V = f(x)$  is the potential on the  $x$  axis,  $V = \text{Re } f(x + jy) = \frac{1}{2}[f(x + jy) + f(x - jy)]$  is the potential throughout the  $x$ - $y$  plane. Furthermore, symmetry of potential about the  $x$  axis implies that  $\partial V / \partial y = 0$  at  $y = 0$ , since the potential and its derivatives are continuous in a charge-free region.

Suppose we were to establish in the region just above the beam in Figure 4.5-3 a potential given by

$$V = \text{Re } A(x + jy)^{4/3} = \frac{A}{2}[(x + jy)^{4/3} + (x - jy)^{4/3}] \quad (4.5-2)$$

This potential has the property that for  $y = 0$  it reduces to  $V = Ax^{4/3}$ , and furthermore that  $\partial V/\partial y = 0$  at  $y = 0$ , so that there would be no transverse force on the electrons at the edge of the beam.

To establish such a potential, the beam-forming electrode must be shaped to conform to an equipotential defined by Equation (4.5-2) and must be operated at that potential. A convenient potential is that of the cathode, since no additional biasing supply is needed in this case. The equipotential corresponding to cathode potential is obtained by setting  $V = 0$  in Equation (4.5-2) and is given by

$$y = (1 + \sqrt{2})x \quad (4.5-3)$$

This is the equation of a straight line making an angle of 67.5 degrees with the  $x$  axis.

Thus, close to the electron beam, the beam-forming electrode makes an angle of 67.5 degrees with the beam edge, since in this region the approximations of a two-dimensional potential and a planar cathode are reasonably valid. The shape of the beam-forming electrode further from the beam and the shape of the anode are so chosen that they produce a potential along the edge of the beam which matches the potential that is characteristic of electron flow between concentric spheres. Often an electrolytic tank<sup>6</sup> is used to determine experimentally suitable electrode contours.

In the region of the anode aperture there is a component of electric field directed toward the axis of the beam, and this acts as a diverging lens. If the anode aperture is small compared with the anode-to-cathode distance, the focal length of this lens is<sup>7</sup>  $4V_{ao}/V'$ , where  $V_{ao}$  is the anode voltage, and  $V'$  is the potential gradient on the cathode side of the anode aperture. (See Problem 3.1.) The lens causes the off-axis electrons to receive a small deflection away from the axis. Beyond the anode aperture, the radial electric field of the beam causes a further deflection of the off-axis electrons away from the axis, with the result that the beam ultimately reaches a minimum diameter and then diverges. If an axial magnetic field is used to confine the beam, the beam would normally be launched into the field near the point of its minimum diameter.

The discussion of Section 4.2 concerning the relationship between anode current and anode voltage for a space-charge-limited diode applies equally well to electron guns such as those illustrated in Figures 4.5-1(a) and 4.5-1(b). Over the range of cathode currents for which space-charge-limited conditions prevail, the beam current varies as the 3/2 power of the

<sup>6</sup>Reference 4a, p. 180.

<sup>7</sup>The effect of the finite size of the anode aperture in Pierce electron guns has been considered by Danielson *et al.*, Reference 4.7, who conclude that in a typical case the focal length given by the above expression should be divided by about 1.1.

anode voltage. Similarly, if the linear dimensions of an electron gun are scaled by a constant factor, the same beam current is obtained for the same applied anode voltage, and the beam dimensions scale with the other linear dimensions of the gun, provided space-charge-limited conditions prevail.

The ratio of beam current to (beam voltage)<sup>3/2</sup> is a constant for any particular electron gun design over the range of beam currents for which space-charge-limited conditions prevail. The ratio is known as the perveance of the gun and is a measure of the amount of beam current the gun can generate for a given applied voltage. If two guns have the same geometry, but differ in their linear dimensions by a constant factor, they both have the same perveance.

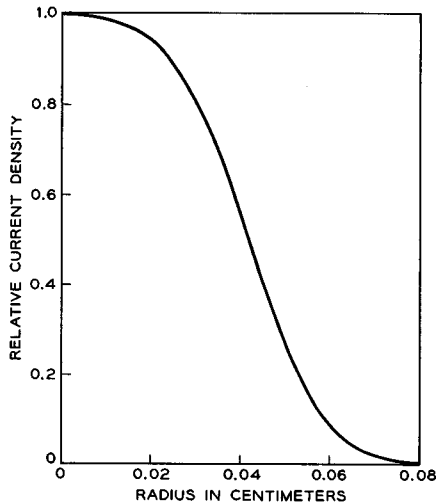


FIG. 4.5-4 Beam current density vs. radial distance from the axis at the point of minimum beam diameter for the electron gun illustrated in Figure 4.5-1(a).

The effects of thermal velocities in Pierce electron guns have been considered by Cutler and Hines,<sup>8</sup> and later by Danielson *et al.*<sup>9</sup> The parameters that apply to the beam at its point of minimum diameter have been summarized in a family of curves by Herrmann.<sup>10</sup> Data concerning the distribution of current density across the beam cross section, the size of the beam at its point of minimum diameter, and the location of the point of minimum

<sup>8</sup>Reference 4.8.

<sup>9</sup>Reference 4.7.

<sup>10</sup>Reference 4.9. See also Reference 4.10.

diameter with respect to the anode aperture can be obtained by reference to the papers by these authors. Figure 4.5-4 shows the calculated current density vs. radial distance from the beam axis at the point of minimum beam diameter for the electron gun illustrated in Figure 4.5-1(a). The curves given by Herrmann also indicate that a nonthermal electron emitted from the edge of the cathode of this electron gun would arrive at the plane containing the minimum beam diameter at a radius of 0.045 cm from the axis. Notice that Figure 4.5-4 indicates that some of the thermal electrons are far beyond this radius when they reach the plane of minimum beam diameter. The beam radius at the cathode is 0.24 cm.

A measure of the distribution of transverse velocities in the beam at the point of minimum diameter can be obtained by assuming that the radial fields acting on the beam between the cathode and the point of minimum diameter are directly proportional to distance from the beam axis.<sup>11</sup> We then can use Equation (4.4-23) to express the probability that an electron at the point of minimum diameter has transverse velocity in the range  $u_t$  to  $u_t + du_t$  as

$$dP(u_t) = \frac{m u_t}{kT} \left( \frac{r_{\min}}{r_c} \right)^2 \epsilon^{-m u_t^2 (r_{\min}/r_c)^2 / 2kT} du_t \quad (4.5-4)$$

where  $r_c$  is the beam radius at the cathode, and  $r_{\min}$  is the beam radius at the point of minimum diameter. This result is sometimes interpreted by saying that the effective "temperature" of the beam generated by the gun is  $(r_c/r_{\min})^2 T$ . For the gun shown in Figure 4.5-1(a) and for a cathode temperature of 1000°K, we can obtain a first-order estimate of the beam temperature at the point of minimum diameter by setting  $r_c = 0.24$  cm and  $r_{\min} = 0.045$  cm, or the minimum distance from the beam axis to the trajectory of a nonthermal electron emitted from the edge of the cathode. The resulting beam temperature is  $(0.24/0.045)^2 \times 1000 = 28,000^\circ\text{K}$ .

The high transverse velocities in a beam generated by a convergent electron gun increase the difficulty of focusing the beam by any of the several methods described in Section 3.4. Higher focusing fields are required to confine the beam to a given diameter than would be predicted by simple theory which assumes laminar electron flow.

In most convergent electron guns, the total beam current determines the cathode area. On the one hand, the cathode emitting surface is characterized by a maximum emission current density consistent with long life of the

---

<sup>11</sup>This assumption implies that the beam current density is uniform over the beam cross section. However, from Figure 4.5-4 it is evident that, in fact, the beam current density at the point of minimum diameter falls off rapidly from a radius about equal to one third the beam radius. Consequently, the estimate of the beam temperature which follows Equation (4.5-4) can only be considered as a first-order estimate.

emitter, so that the total beam current determines the minimum cathode area consistent with long cathode life. On the other hand, a larger cathode area than necessary would be wasteful of heater power, and the transverse velocities in the beam for a given minimum beam diameter would be unnecessarily high.

Some reflex klystron oscillators require high-current, high-current-density beams at relatively low voltages, often a few tens of milliamperes at a few hundred volts. Electron guns which produce these beams are of much higher perveance than the gun illustrated in Figure 4.5-1(a). One way to increase the perveance of an electron gun is to reduce the anode-to-cathode spacing. This, in turn, necessitates opening the anode aperture in order to pass the beam. However, it is found that, if the diameter of the anode aperture approaches half the anode-to-cathode spacing, the potential at the center of the aperture falls sufficiently below anode potential that the spherical diode is no longer approximated. In this case, the current density drawn from the edge of the cathode is greater than that drawn from the center of the cathode, and spherical aberration in the accelerating field introduces relatively high transverse velocities in the beam. Furthermore, it can be shown that, if the ratio  $\bar{r}_c/\bar{r}_a = (\text{radius of cathode emitting surface measured from the center of curvature of the emitting surface})/(\text{distance from anode aperture to the center of curvature of the cathode emitting surface})$  is reduced below 1.4, the lens at the anode aperture becomes sufficiently strong that the beam beyond the anode is divergent.

Higher perveance also can be obtained by maintaining a relatively large  $\bar{r}_c/\bar{r}_a$  and by increasing the angle of convergence (i.e., the angle subtended by a diameter of the cathode at the center of curvature of the cathode emitting surface). This is the approach used in the electron gun shown in Figure 4.5-1(b). The angle of convergence in this case is 145 degrees, or nearly 6 times that of the gun shown in Figure 4.5-1(a). However, the anode aperture is still relatively small, and, in fact, the anode is shaped to follow the beam contour. Although an appreciably higher perveance is obtained in this manner, spherical aberration in the accelerating field causes many of the electrons emitted from the edge of the cathode to cross the axis of the beam near the point of minimum diameter. As a consequence of this, the electron flow is far from laminar, and the transverse velocities are large. The beam is therefore difficult to confine with a magnetic field. The use of even higher angles of convergence would lead to still greater transverse velocities, and few applications could use such a gun.

Figure 4.5-5 shows a plot of beam current vs. anode voltage for the gun shown in Figure 4.5-1(b). The plot is made on "two-thirds power" paper in which the ordinate scale is proportional to the  $3/2$  power of linear distance measured up the page from the origin, while the abscissa scale is linear. The

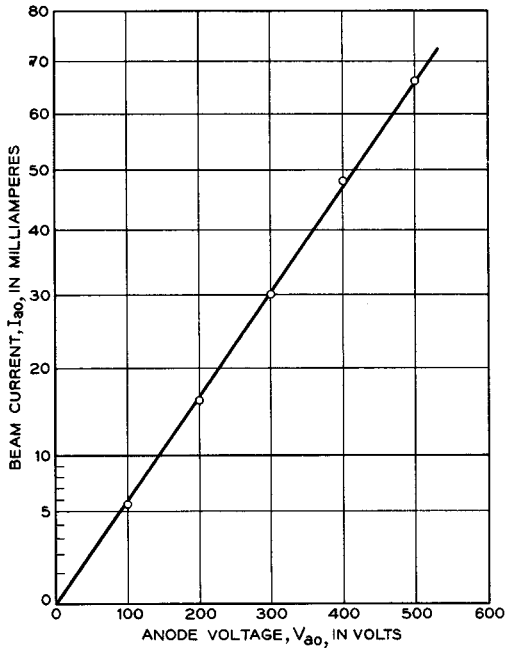


FIG. 4.5-5 A plot of beam current vs. anode voltage for the gun shown in Figure 4.5-1(b).

straight-line relationship between  $I_{ao}$  and  $V_{ao}$ , when plotted on this paper, implies that  $I_{ao}$  is proportional to  $V_{ao}^{3/2}$ , as we would expect from our earlier discussion.

Figure 4.5-1(c) illustrates an electron gun which is used in a low-noise traveling-wave amplifier. The gun is operated in a uniform axial magnetic field of 0.06 weber/meter<sup>2</sup>, and the electron motion is similar to that described in Section 3.4(b) under the heading of Confined Flow. Several apertured accelerating electrodes are provided. The potentials of these electrodes are adjusted to minimize the amplitude of noise signals excited in the electron beam by statistical fluctuations in the electron emission velocity and current at the cathode. (The reduction of noise in an electron beam by this method is described in Chapter 13.) The uniform axial magnetic field might be provided by the permanent magnet circuit illustrated in Figure 1.5-6.

The cathode of the gun illustrated in Figure 4.5-1(c) is planar and of diameter 0.63 mm. A beam current of 0.5 milliamp is drawn from the cathode, and the cathode current density is 160 ma/cm<sup>2</sup>. As the beam

leaves the cathode, its diameter shows a slight increase because of transverse emission velocities and radial fields in the accelerating region. However, the axial magnetic field confines the beam diameter sufficiently that the beam can pass through a helix-type slow wave circuit of inside diameter 1.3 mm and length 13 cm with less than 0.5 microamp interception.

### b. *Electron Guns for Cathode-Ray Tubes and Storage Tubes*

These electron guns focus the beam to a crossover which is imaged onto the screen or storage surface by a lens beyond the crossover. Often an apertured electrode between the crossover and the lens passes only the central portion of the beam, so that the effects of aberrations in the gun and lens are small.

Generally the beam currents incident upon the screen or storage surface are lower than those used in microwave tubes. Storage tubes that make use of secondary emission from insulating materials often employ beams of a few microamperes at one or two thousand volts; cathode-ray tubes frequently employ beam currents of a few tens of microamperes at several thousand volts, perhaps 2 to 6 thousand volts; whereas the beam incident upon the screen of a television tube often amounts to a few hundred microamperes at 15 to 20 kv.

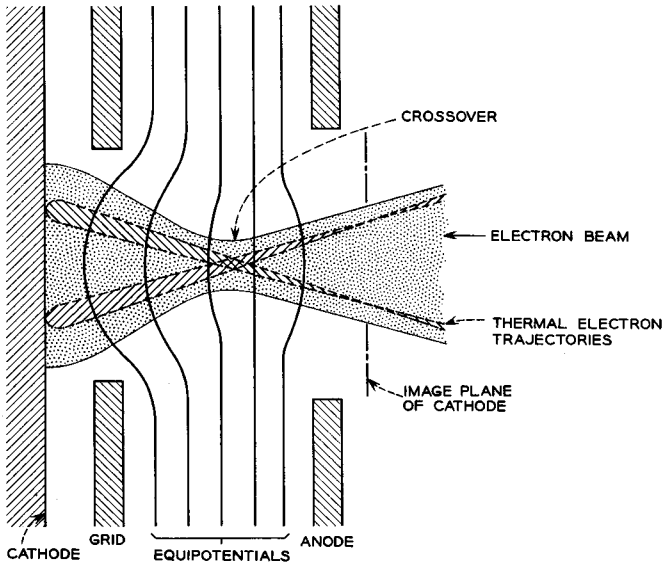


FIG. 4.5-6 A triode electron gun such as is used in a cathode-ray tube or storage tube.



The crossover is formed by a "triode" system consisting of a cathode, a "grid," and an anode, the grid and anode each having a single aperture. Such a structure is illustrated in Figure 4.5-6. The grid is always biased negatively with respect to the cathode, and consequently the current drawn from the cathode comes from a small circular area opposite the grid aperture. Equipotentials plotted in the figure show that electrons passing through the grid aperture experience a field which is both accelerating and convergent. The convergent field causes the nonthermal electrons to cross the axis between the cathode and the anode, and in this way the crossover is formed. Beyond the anode, the paths of the thermal electrons emitted from a single point on the cathode cross one another, and an image of the cathode is formed. The system is sometimes called an *immersion* lens, since the cathode is "immersed" in the accelerating field.

In the region of the crossover, the beam diameter reaches a minimum. The size of the minimum beam diameter is affected by three principal factors: Thermal emission velocities at the cathode, the accelerating potential, and aberrations in the convergent field which forms the crossover. Space charge may also affect the beam diameter at the crossover if the beam current is high and the beam voltage is low. If the convergent field were aberration-free, and if space-charge effects were small, the nonthermal electrons emitted from all parts of the cathode surface would cross the axis at essentially the same point. In this case, we might further assume that a thermal electron passing the crossover would be displaced from the axis by a distance proportional to its initial transverse velocity and independent of its point of emission on the cathode. Suppose that an electron emitted from the cathode with transverse velocity equal to  $\sqrt{kT/m}$  were displaced a distance  $\sigma$  from the axis by the time it reached the crossover. Then, using the arguments presented in connection with Equations (4.4-2) and (4.4-3), it is easily shown that the current density in the region of the crossover would be proportional to  $e^{-r^2/2\sigma^2}$ , where  $r$  is the distance from the axis to the point where the beam current density is determined. If the lens system beyond the crossover is aberration-free, and if the beam is focused to a second crossover at the screen, the current density incident upon the screen is also of this form, but with a  $\sigma$  increased by the magnification of the lens.

If the grid is made sufficiently negative, the beam current is cut off. Clearly the cutoff condition will prevail when the off-cathode potential gradient at a point on the cathode surface directly opposite the center of the grid aperture is zero or negative. Figure 4.5-7(b) shows a plot of the grid cutoff voltage vs. anode voltage for the triode shown in Figure 4.5-7(a). The straight-line relationship can be explained by noting that the net off-cathode potential gradient is a superposition of that caused by the grid and that caused by the anode, so that doubling the anode voltage requires

double the grid voltage in order to keep the off-cathode potential gradient at the center of the cathode equal to zero. The slope of the line, of course, is dependent upon the electrode dimensions and spacings.

The difference between the applied grid voltage and the cutoff voltage is called the grid drive voltage. As the grid is made more positive than cutoff, the area of the region of the cathode from which current is drawn increases, and the current density drawn from regions of the cathode surface which are already contributing to the beam current increases. Figure 4.5-7(c) shows

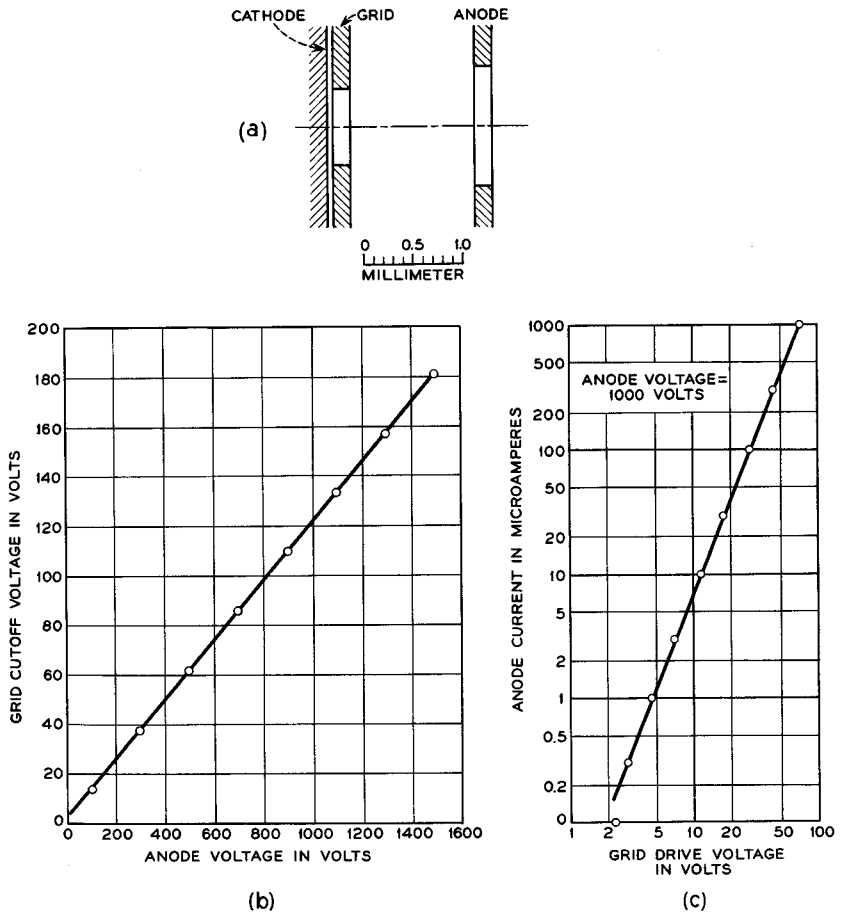


FIG. 4.5-7 Plots of grid cutoff voltage vs. anode voltage and beam current vs. grid drive for the triode gun structure shown in part (a) of the figure.

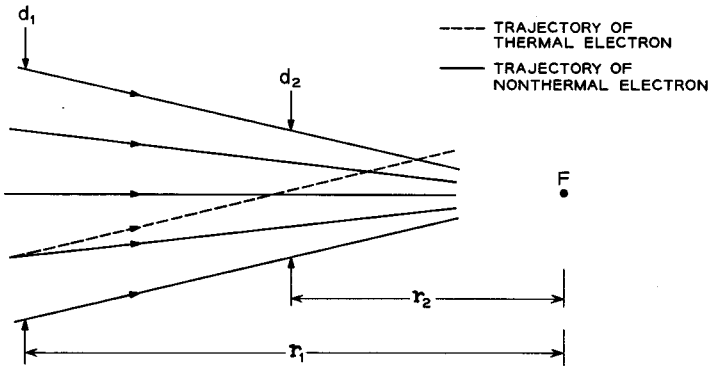
a plot of beam current vs. grid drive voltage for the triode shown in Figure 4.5-7(a). The slope of the straight-line relationship indicates that the beam current of this structure increases as about the 2.4 power of the grid drive voltage over the range of values for which the data are plotted.

Many experimental data concerning relationships between design parameters and the electrical performance of electron guns for cathode-ray tubes and storage tubes are presented in an informative paper by Hilary Moss.<sup>12</sup>

**PROBLEMS**

4.1 For the conditions of applied anode voltage and cathode emission illustrated in Figure 4.1-1(d), show that the time taken for an electron to travel from the cathode to the anode of a planar diode is 3/2 as great as the time taken when no space charge is present. Assume zero emission velocity and  $dV/dx = 0$  at the cathode.

4.2 The 3/2 power law of anode current vs. anode voltage does not apply to a diode operating under temperature-limited conditions. Explain why the arguments presented in Section 4.2 are not applicable in this case.



**Problem 4.3**

4.3 The figure shows a beam of electrons which is convergent upon the point *F*. The trajectories of several nonthermal electrons and one thermal electron are shown in the figure. The beam current density is assumed to be small, and no external fields are applied in the region of the beam. From geometrical considerations show that the thermal electron crosses the nonthermal electron trajectories with a transverse component of velocity which varies inversely as the beam diameter, and hence that

$$u_{t2} = \frac{\bar{r}_1}{\bar{r}_2} u_{n1} = \frac{d_1}{d_2} u_{n1}$$

<sup>12</sup>Reference 4e.

where  $u_{t1}$  and  $u_{t2}$  are, respectively, the transverse velocity of the thermal electron relative to the nonthermal electron trajectories at the points where the beam diameter is  $d_1$  and  $d_2$ , respectively.

### REFERENCES

Three general references on electron guns are:

- 4a. J. R. Pierce, *Theory and Design of Electron Beams*, 2nd Ed., D. Van Nostrand Co., Inc., Princeton, N. J., 1954.
- 4b. C. Suskind, *Advances in Electronics and Electron Physics* **VIII**, 363, 1956.
- 4c. O. Klemperer, *Electron Optics*, 2nd Ed., Chapter 9, Cambridge University Press, Cambridge, England, 1953.

The following two papers describe electron guns for cathode-ray tubes. Many data of a practical nature are given in the second paper.

- 4d. H. Moss, *J. British IRE* **5**, 10, 1945.
- 4e. H. Moss, *J. British IRE* **6**, 99, 1946.

Other references covering specific items discussed in the chapter are:

- 4.1 I. Langmuir and K. T. Compton, *Revs. Modern Phys.* **3**, 191, 1931.
- 4.2 I. Langmuir and K. Blodgett, *Phys. Rev.* **22**, 347, 1923.
- 4.3 I. Langmuir and K. Blodgett, *Phys. Rev.* **24**, 49, 1924.
- 4.4 J. R. Pierce, *J. Appl. Phys.* **10**, 715, 1939.
- 4.5 D. B. Langmuir, *Proc. IRE* **25**, 977, 1937.
- 4.6 J. R. Pierce, *J. Appl. Phys.* **11**, 548, 1940.
- 4.7 W. E. Danielson, J. L. Rosenfeld, and J. A. Saloom, *Bell System Tech. J.* **35**, 375, 1956.
- 4.8 C. C. Cutler and M. E. Hines, *Proc. IRE* **43**, 307, 1955.
- 4.9 G. Herrmann, *J. Appl. Phys.* **28**, 474, 1957.
- 4.10 P. T. Kirstein, *IEEE Trans. on Electron Devices*, Vol. ED-10, 69, 1963.